4 Galactic Rotation Curves

While the $M_{<8.5\mathrm{kpc}}$ estimate compares well with the luminous matter within the **solar circle**, i.e. 8.5 kpc, it is much less than the mass estimate obtained from **Galactic rotation curves**, the focus here. Observational mapping of radial v_r and transverse v_t velocities as functions of distance and galactic longitude yields maps of the Galactic orbital or angular velocity functions: **C & O, pp. 915–19**

$$\Theta(R) \quad \text{or} \quad \Omega(R) \;\equiv\; \frac{\Theta(R)}{R} \quad . \tag{16}$$

Generally, determination of v_r is easier, using line-of-sight Doppler shift information. Then, for stars far enough away to not discern their proper motions on the sky, the sky-plane component v_t is estimated via $\sigma_t^2 \sim 2\sigma_r^2$. This assumes that stellar proper motions are isotropic and virialized.

The geometry for analyzing the differential rotation of the Galactic plane. The sun as it point *O*, the Galactic center is at point *C*, and the star of interest is at point *S* and at a distance *d* from the sun.
R_0 = 8.5 kpc.

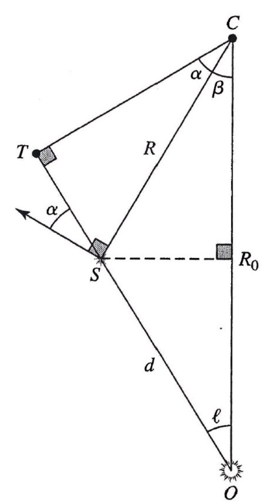

• In the local neighbourhood, the rotation function $\Omega(R)$ can be expanded as a Taylor series, leading to an approximate form for the velocity components as a function of galactic longitude ℓ:

$$v_r \;\approx\; Ad\,\sin 2\ell \quad , \quad v_t \;\approx\; Ad\,\cos 2\ell + Bd \quad . \tag{17}$$

Velocity components are only as accurate as the distance determination technique. The 180° period in ℓ is distinctive. These forms are only valid for the solar neighbourhood, and were derived by Jan Oort in 1927.

• The coefficients A and B are known as **Oort's constants**, given by

$$\begin{aligned} A &\equiv -\frac{1}{2}\left\{ \frac{d\Theta}{dR}\bigg|_{R_0} - \frac{\Theta_0}{R_0} \right\} \approx 14.8 \pm 0.8 \text{ km sec}^{-1} \text{ kpc}^{-1} \\ B &\equiv -\frac{1}{2}\left\{ \frac{d\Theta}{dR}\bigg|_{R_0} + \frac{\Theta_0}{R_0} \right\} \approx -12.6 \pm 0.6 \text{ km sec}^{-1} \text{ kpc}^{-1} \quad . \end{aligned} \tag{18}$$

The measured values are based on results from the Hipparcos astrometry mission of the early 1990s.

[*Reading Assignment: Detailed derivation of Oort's Constants: pp. 908–911*]

• Ensembles of individual stars are perhaps more unwieldy for use in determining the **galactic rotation curve**, i.e. $\Omega(R)$. Neutral hydrogen gas mapping is much more facile, since 21 cm line radiation easily penetrates the Galactic center region. Accordingly, 21cm radial velocity profiles are rich in the information concerning the rotation curve.

Plot: Sample 21cm Radial Velocity Profile and Associated Geometry

$*$ For longitudes $0° < \ell < 90°$ and $270° < \ell < 360°$, the convolution of Doppler redshift and blueshift with distance from the sun is relatively straightforward. For other longitudes, only the outer galaxy is sampled.

$*$ The maximal radial velocity arises at the tangent point, corresponding to the minimum distance from the GC along a particular line of sight. This gives a unique mapping of $\Omega(R)$ for $R \leq R_0$.

Sample 21cm Radial Velocity Profile

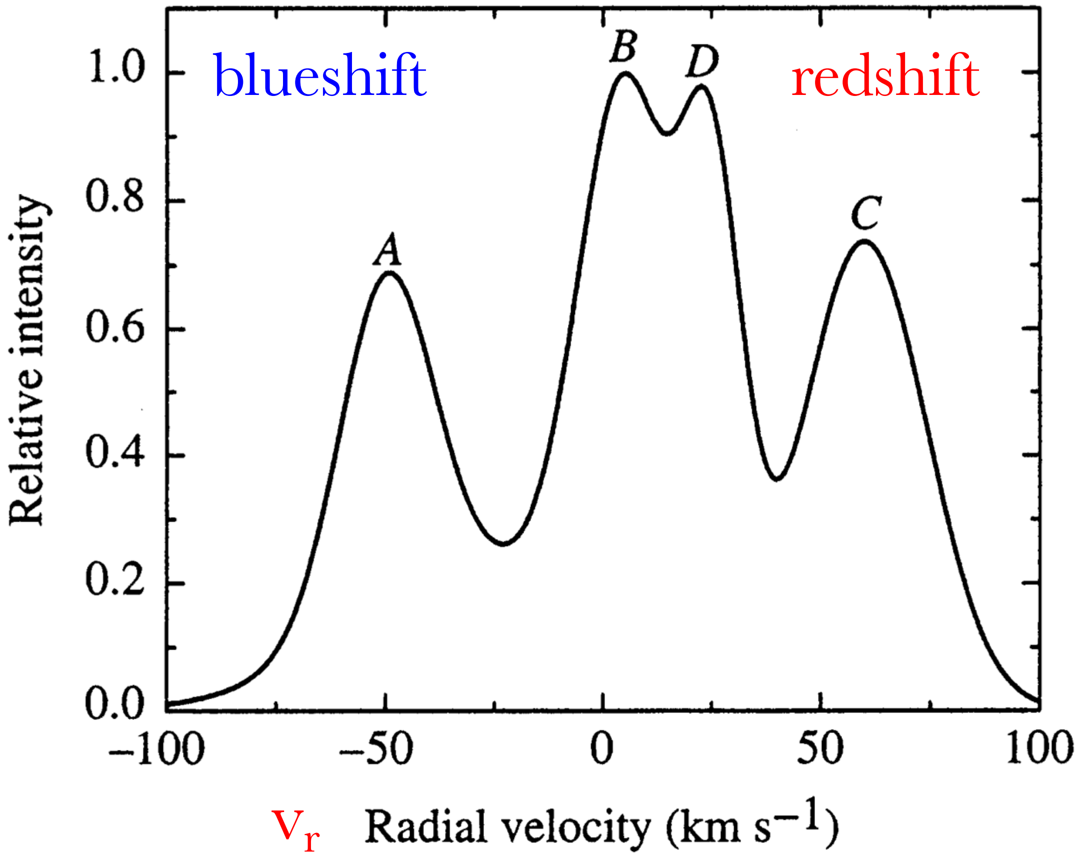

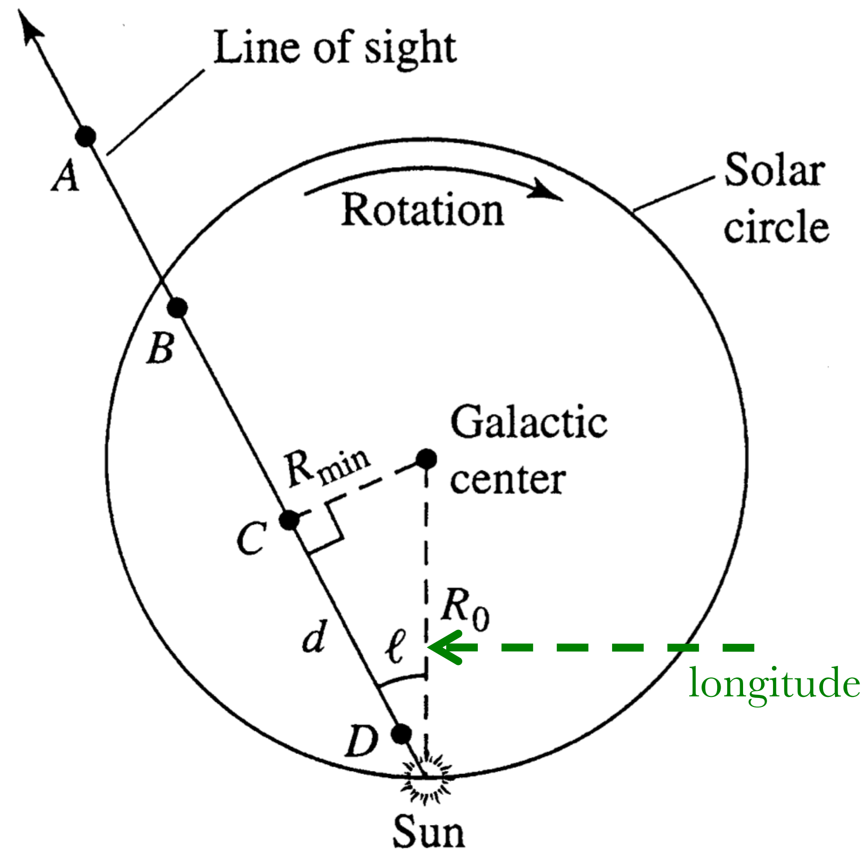

- *Left*: a typical 21cm HI line profile with $v_r = (\Delta\lambda/\lambda)\, c$. [From Carroll+Ostlie]
- *Right*: geometry for which the line profile is produced by observing several gas clouds along a particular line of sight with longitude *l*. Because of Galactic rotation, each cloud has a different radial velocity relative to the Sun's motion.

4.1 Evidence for Dark Matter

Assembling the information on HI, CO, stars etc, one arrives at the rotation curve for the Milky Way

Plot: The Rotation Curve of the Milky Way Galaxy

- The surprise is that it does not obey a Keplerian form at large distances R from the GC. From Eq. (15), i.e., $M = \Theta^2 R/G$, we would infer

$$\Theta \;\propto\; \frac{1}{\sqrt{R}} \quad \Leftrightarrow \quad \Omega \;\equiv\; \frac{\Theta(R)}{R} \;\propto\; \frac{1}{R^{3/2}} \quad . \tag{19}$$

This implies the existence of non-luminous matter on large scales, well beyond the solar circle. This indicates a high mass-to-light ratio, typically of the order of $\gtrsim 10^3 M_\odot/L_\odot$ (around 1400 time solar from Schecter's galaxy studies). The gravitating matter is then termed **dark matter**.

$*$ Velocities mark an *isothermal sphere* of galactic matter.

$*$ Rotation curves for other spiral galaxies are similarly **flat** $\Rightarrow$ dark matter is common in the nearby universe; this extends to cosmological scales.

$*$ The rapid rise of Θ (in km/sec) within the outer bulge is quasi-**rigid-body rotation**, since $\Theta \propto R$ (approximately) and Ω is constant.

- Using the enclosed mass result $M = \Theta^2 R/G$, we can differentiate to derive $dM/dR = \Theta^2/G$. Clearly, velocities yield the mass gradient information. Imposing mass conservation in a *spherically-symmetric* system,

$$\frac{dM}{dR} \;=\; 4\pi R^2 \rho(R) \;=\; \frac{\Theta^2}{G} \quad . \tag{20}$$

It then follows that the mass density profile is uniquely specified in terms of the galactic rotation curve, via

$$\rho(R) \;=\; \frac{\Theta^2}{4\pi G R^2} \quad . \tag{21}$$

The $1/R^2$ density profile is much shallower than the observed stellar density profile in the disk, which is $\sim R^{-3.5}$. A cylindrical profile is $\sim 1/R$.

Rotation Curve of Milky Way

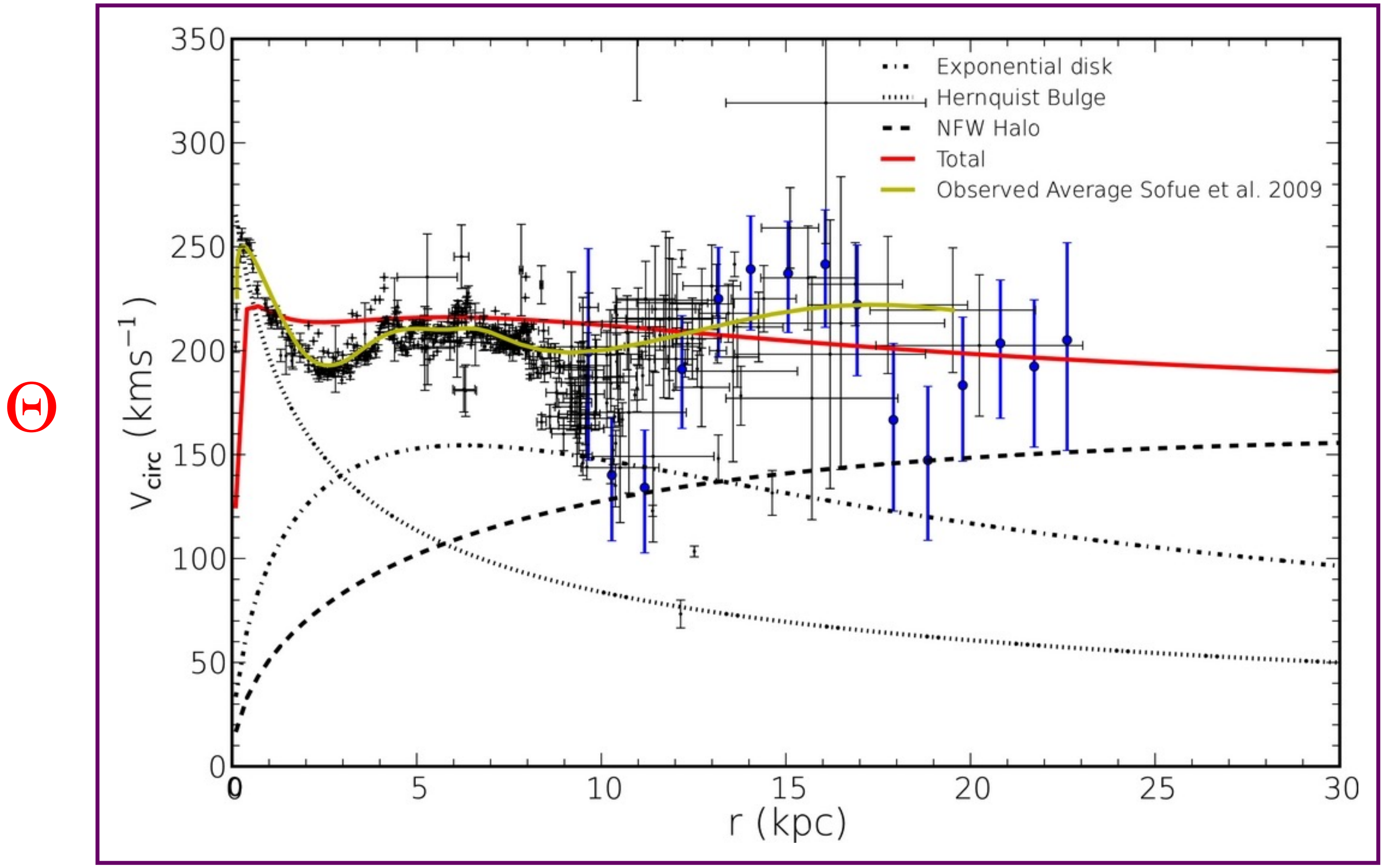

- Kinematic rotation curve of the Milky Way using blue horizontal branch stars from the Sloan Digital Sky Survey (SDSS).
- From Kafle et al. (2012 *ApJ* **761**, 98). A similar result is obtained much earlier in CO/HI mapping of Clemens (1985, *ApJ*, **295**, 422).

A commonly-assumed spherically-symmetric density profile for dark matter is $\rho(R) = \rho_0/[1 + R^2/a^2]$ for some fall-off radial scale a. Using simulations of **cold, dark matter** (CDM), Navarro, Frenk & White (1996) determined that the density profile is closely approximated by a universal form

$$\boxed{\rho_{\rm NFW}(R) \;=\; \frac{\rho_0}{R/a\,[1 + R^2/a^2]} \quad .} \tag{22}$$

∗ This form is integrably-convergent at small radii in the bulge, even though there is a **density cusp** at $R = 0$.

It is, however, logarithmically divergent at large radii, since it falls off as $1/R^3$. On these scales, dark matter halos of neighbouring galaxies merge. The DM halo extends out to at least 230 kpc, and constitutes some 95% of the mass of the Milky Way.

• One leading candidate for the DM is from particle physics – **weakly-interacting massive particles** (WIMPS), nonbaryonic matter that does not readily exhibit electromagnetic signatures that we might see.

∗ Exotic particle decays (or collisions) yielding photons are the most promising detection avenue for WIMPs, and for appropriate masses, these emerge in the gamma-ray band. This defines an agenda for NASA's *Fermi* mission.

• Another candidate is **massive compact halo objects** (MACHOs), such as white dwarfs, neutron stars, black holes or brown dwarf stars. Evidence for their existence in the halo comes from gravitational (GR) microlensing, a technique pioneered in the early 1990s.

Plot: Achromatic Light Curves for Gravitational Microlensing Events

∗ Such lensing focuses light and so amplifies the intensity as the lens passes in front of a distant source. Yet the occurrence rate of such microlensing events is far too low to account for a major portion of the dark matter halo.

Light Curve for MACHO Passage

- A MACHO lensing event towards Andromeda (M31). Observed in two bands (R and I), it is *achromatic*. Solid curve is model with finite source extent included. Bottom panel is residuals between photometry data and model. Calchi Novati et al. (2010, ApJ 717, 987).
- See Alcock et al. (1993, Nature 365, 621) for seminal MACHO discover paper.
- Byproducts of MACHO searches in LMC and SMC include discovery of RR Lyrae and Cepheid variables.

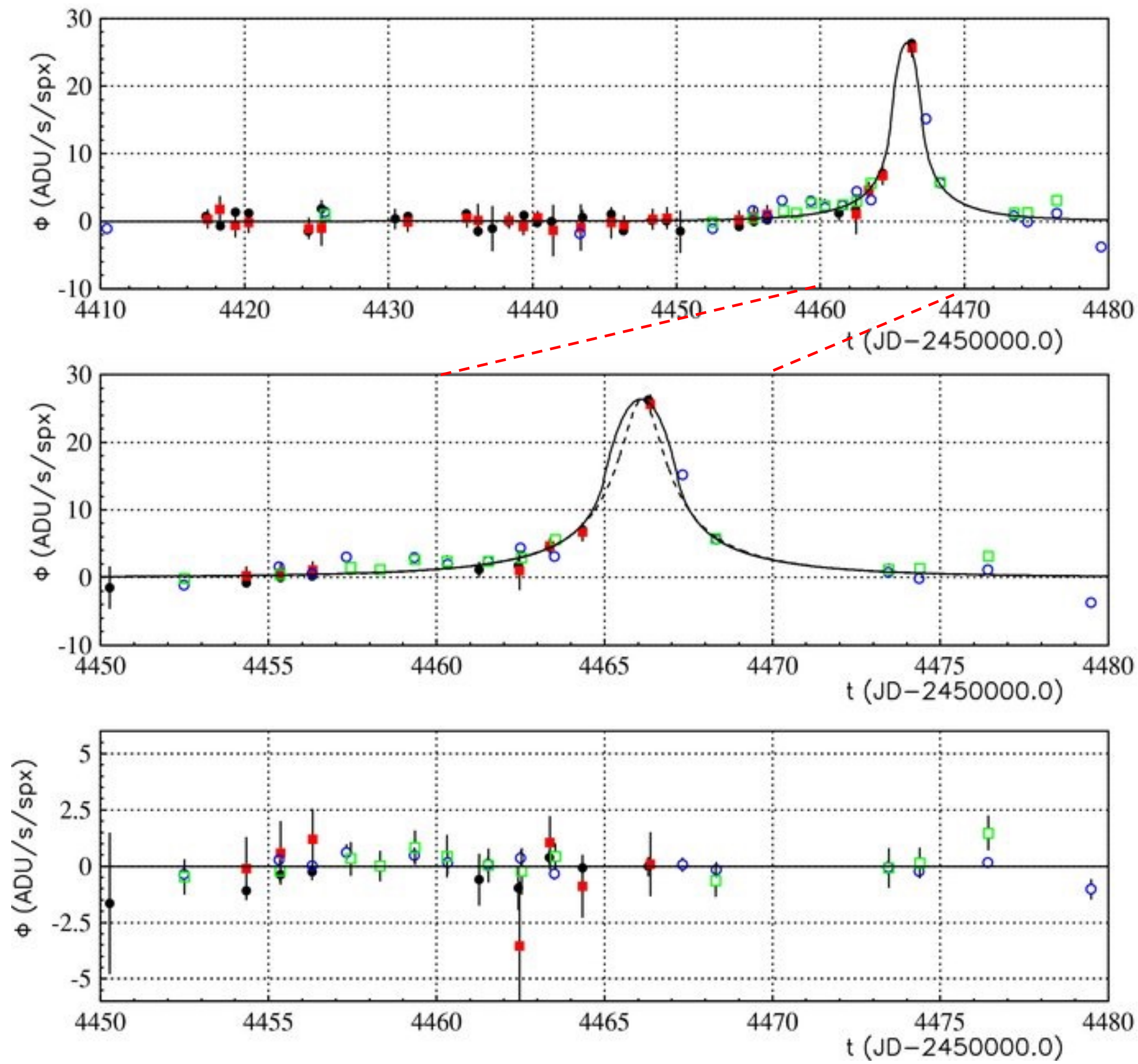

5 The Galactic Center

• The Galactic Center (GC) region around Sgr A* is a rich astronomical environment. Stars in the central few parsecs are probed in the IR at typically 2.2μ m, the so-called **K-band**. This permits penetration through the dust that obscures the optical, and picks out K and M stars. **C & O, Sec. 24.4**

∗ There is a central cluster of stars that exhibits an apparent rise in density as $r^{-1.8}$ as the radius drops from $r = 1\,\text{pc}$ to $r = 0.1\,\text{pc}$. The center of this cluster has been resolved, leading to the inference of a massive central body.

∗ Gravitational collisions between stars arise in Myr timescales [this will be explored more in the Galaxies Chapter], so that relaxation to an isothermal distribution is rapid. This should display a r^{-2} density distribution, as discussed above for the rotation curve, which is close to the value observed.

• The central cluster is a site of star formation, and inferences of this are drawn from a key piece of evidence that supernovae have been repeatedly occurring. There is a diffuse cloud of 511 keV gamma-ray radiation in the GC region, and this is generated by the annihilation of non-relativistic positrons via $e^+ + e^- \to \gamma\gamma$. The prime candidate for generating such positrons is nucleosynthetic β decays (e.g. Ni, Co) associated with supernovae.

Plot: 511 keV Diffuse Emission from Galactic Center Region

• Radio observations are also penetrating. Karl Jansky was the first to locate a radio source in the direction of Sagittarius, in the 1930s, before radio astronomy took off. HI cloud observations reveal a **nuclear disk** on scales of 1 kpc, tilted with respect to the galactic plane.

• On much smaller scales, 20cm continuum (synchrotron) observations indicate the presence of a compact central nebula now called **Sagittarius A**, and an extended arm, and an oblique filament.

Plot: 20cm Synchrotron Emission Map of Sagittarius A

This nebula is likely associated with a central supermassive black hole.

Galactic Center in 511 keV Emission

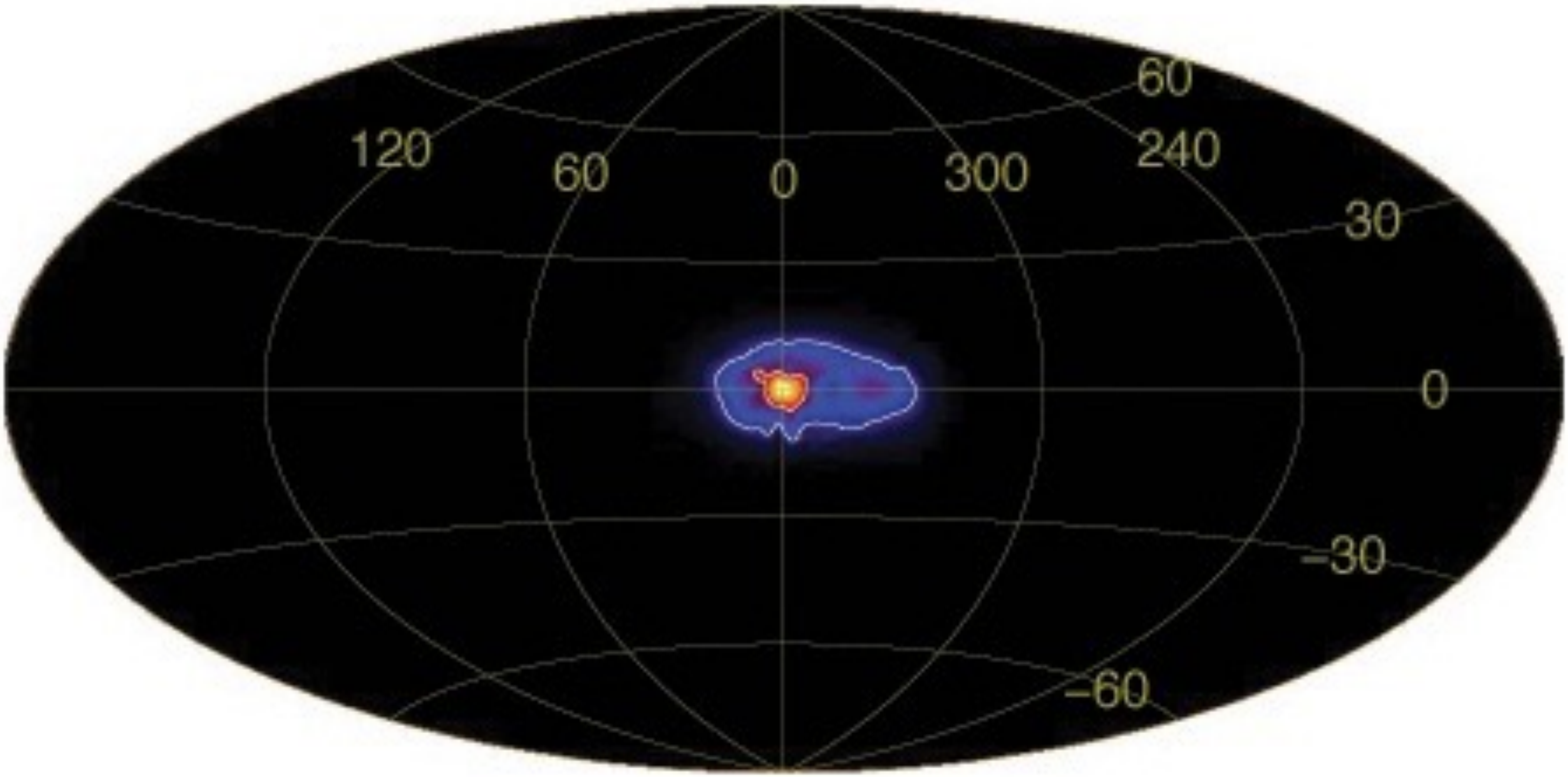

- *INTEGRAL* IBIS map of 511 keV e^+e^- annihilation line emission. Positrons come mostly from SNe decay channels and collide with ambient electrons. The temperature of the e^+ is around 3 keV.

Galactic Center in Radio

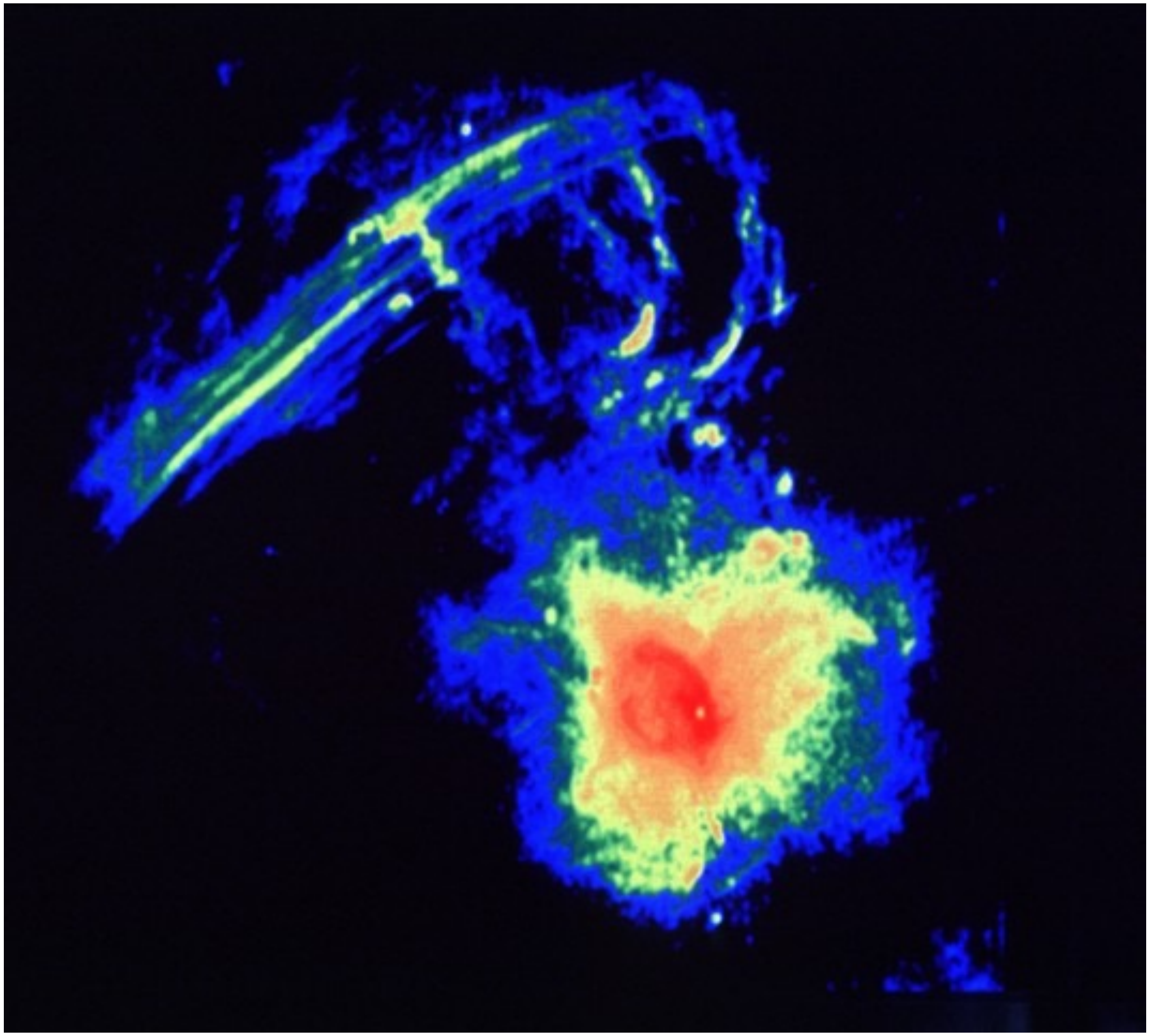

From NRAO Image Gallery

- 20cm continuum synchrotron emission map from VLA in Sagittarius A region.
- The compact central nebula and extended arm and filament are pronounced.

∗ The central nebula actually takes the shape of a **molecular circumnuclear ring** extending between radii of 2pc and 8pc. HI and CO line observations confirm that the ring rotates almost as a rigid body at a speed of 110 km/sec — again suggesting the presence of a compact central, massive body. The ring has a mass of around $1 - 3 \times 10^4 M_\odot$.

• Other structure includes **Sgr A East**, a supernova remnant. There is also a compact X-ray source coincident with **Sgr A***, of X-ray luminosity 10^{35} erg/sec in the 2–6 keV band (**soft X-rays**) and 2×10^{38} erg/sec in the 10 keV – 1 MeV band (**hard X-rays**).

• A more recent discovery that is not spatially located in the GC region, but possibly physically connected to it is of the tenuous, diffuse gamma-ray clouds discovered at high Galactic latitudes by NASA's *Fermi* telescope. These large regions, around 7-8 kpc in diameter, straddle the GC and the inner disk in an approximately symmetrical manner (Meng et al., ApJ 2010).

Plot: Fermi Bubbles and gamma-ray emission from the Galactic disk

• The gamma-rays from the Fermi Bubbles are more energetic on average than those from the Galactic disk, both being generated by high-energy, non-thermal ions and electrons known as **cosmic rays** that collide with gas and dust. The cosmic rays in the Bubbles may originate from **Sgr A***.

[*Reading Assignment: X-ray and 511 keV and 1.8 MeV gamma-ray sources near the Galactic Center: pp. 932–32*]

Gamma-Ray Diffuse Emission: Fermi Bubbles

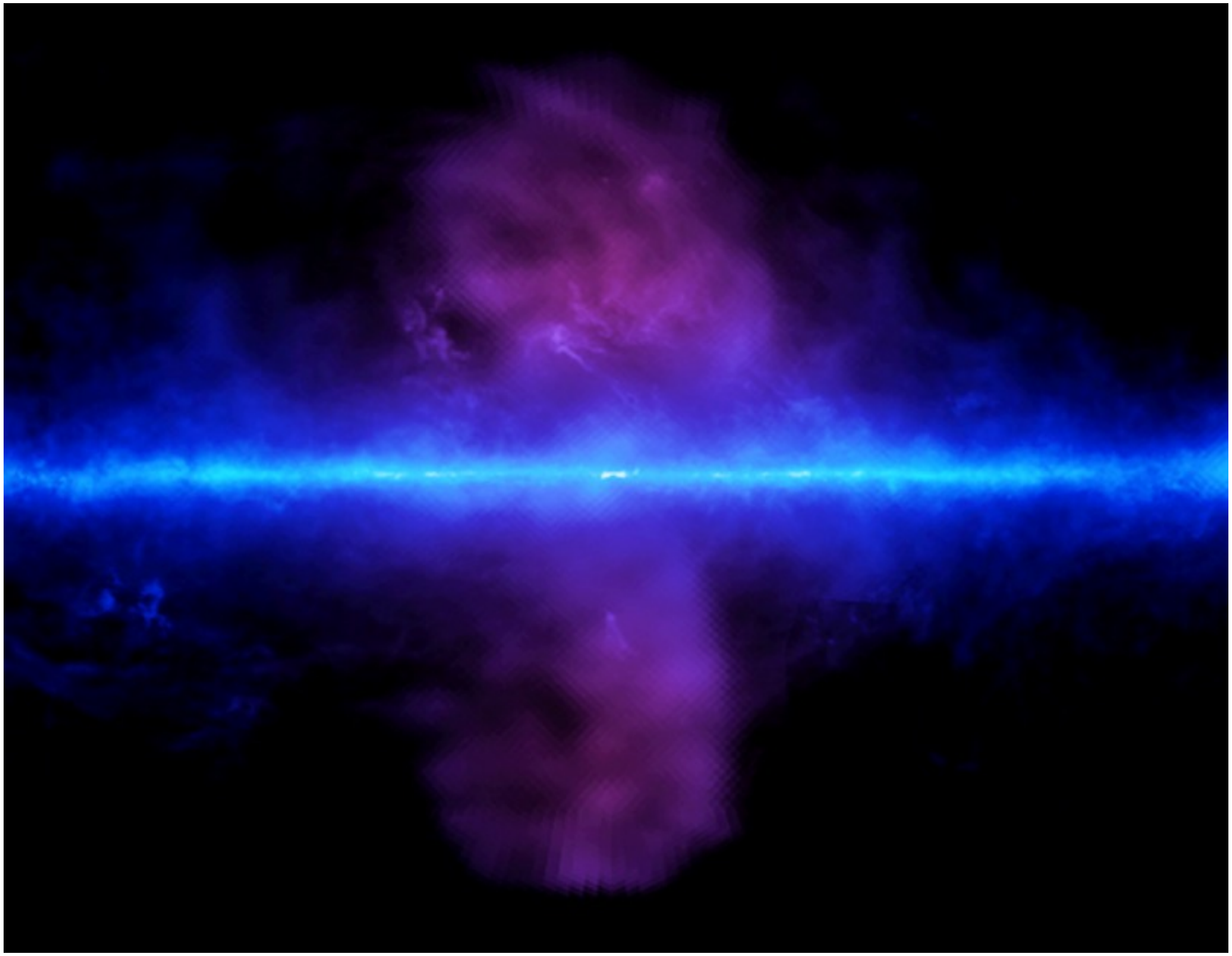

See Meng et al. (ApJ 724, 1044; 2010)

- Galactic diffuse emission above 100 MeV (blue) together with high-latitude *Fermi* Bubbles (purple), all detected by the *Fermi* Large Area Telescope.
- From https://fermi.gsfc.nasa.gov/science/constellations/pages/bubbles.html